Searches for 3rd generation SUSY-partners

Term Paper: "Particle Physics at the LHC"

Simeon Schrott

July 8, 2014

Contents

1 Introduction

Over the past decades different models tried to give an explanation to observations of experiments done with particle accelerators. The Standard Model (SM) survived all these experiments and is able to describe all events produced with accelerators. But there are several problems which the SM is not able to solve, like: the Problem of Mass, the Problem of Flavour and the Problem of Everything and open questions like: What is dark matter or dark energy or is there an unification at a certain energy scale (GUT-scale)? Possible models able to give solutions to most of those questions are *Supersymmetry*-extensions of the SM [1, p. 1,15].

1.1 What is *Supersymmetry*?

Introducing supersymmetric (SUSY) extensions to the SM applies a symmetry linking bosons and fermions using a spin-$\frac{1}{2}$ charge. This leads to symmetries generated not only by bosons but also by fermions [1, p. 17] and within those models the conservation of lepton number and baryon number is violated and a new preservative quantum number is introduced, the R-parity. The R-parity is defined as follows (eq. 1) [2, p. 16], B is the baryon number, L the lepton number and S the spin of the particle.

$$R = (-1)^{3(B-L)+2S} \begin{cases} +1 & \text{, SM-particles} \\ -1 & \text{, SUSY-particles} \end{cases} \tag{1}$$

From R-parity follows that SUSY-particles are produced in pairs, one SUSY-particle decay in an odd number of SUSY-particles and the lightest SUSY-particle is stable, often called the LSP ("lightest supersymmetric particle"). The LSP is a candidate for cold dark matter if it is electric- and colour-charge free [1, p. 30]. From observations in experiments done so far in high energy physics it is clear that the supersymmetry must be a broken symmetry, otherwise one would have observed the sparticles at the same masses as the corresponding particles.

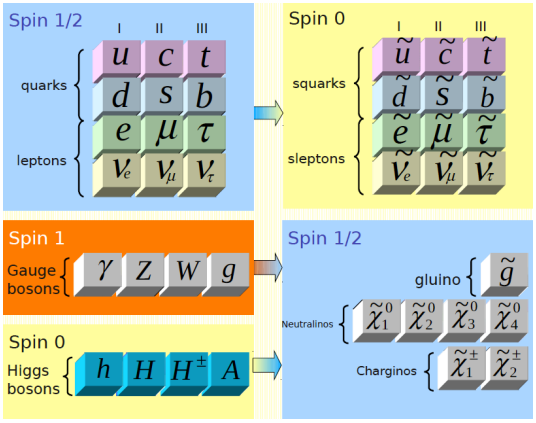

Figure 1: All particles given by the MSSM. To differ between SM-particles and SUSY-particles, SUSY-particles get a "s" ahead the name of the corresponding SM-particle and a tilde above the short cut [3, p. 37].

One supersymmetric extension is called "Minimal Supersymmetric Extension of the Standard Model" (MSSM). In this model one SUSY-particle is postulated to each SM-particle with the same quantum numbers except the spin. Also there are the same gauge interactions. Figure 1 shows all particles contained in this model. To differ between SM-particles (particles) and SUSY-particles (sparticles), sparticle scalars get a "s" ahead the name of the corresponding SM-particle (squark, stop, sfermion, ...), to sfermions the suffix "ino" is attached (gaugino, higgsino, wino, ...) and a tilde above the short cut of the particle indicates the corresponding sparticle.

In the following, two searches will be presented trying to find evidence to direct stop (3rd generation sparticle) pair production which will then decay further into known particles and the lightest neutralino which is considered to be the LSP. The first search will consider all-hadronic final states and the second search only uses final states with one lepton.

2 Motivation

The motivation for searches after the 3rd generation sparticles is based on the fact that in many supersymmetric models the 3rd generation sleptons and squarks are predicted to be the lightest ones. For sfermions this can be easily seen by looking at the mass matrices in the base of the chiral eigenstates $\{\tilde{f}_L, \tilde{f}_R\}$, where $\tilde{f}_{L,R}$ are the superpartners of the left- and the right-handed fermions $f_{L,R}$. The mass matrix for a sfermion in this particular base is of the form [1, p. 24,25]:

$$M^2_{\tilde{f}} \equiv \begin{pmatrix} m^2_{\tilde{f}_{LL}} & m^2_{\tilde{f}_{LR}} \\ m^2_{\tilde{f}_{LR}} & m^2_{\tilde{f}_{RR}} \end{pmatrix} \tag{2}$$

The off diagonal takes the form:

$$m^2_{\tilde{f}_{LL,RR}} = m^2_{\tilde{f}_{L,R}} + m^{D^2}_{\tilde{f}_{L,R}} + m^2_{\tilde{f}} \tag{3}$$

$$m^2_{\tilde{f}_{L,R}} = m_f \left(A_f + \mu^{tan\beta}_{cot\beta} \right) \tag{4}$$

Here $m^2_{\tilde{f}_{L,R}}$ is the soft supersymmetry-breaking mass and m_f represents the mass of the corresponding fermion. The contribution from the quartic D terms in the effective potential is represented through $m^{D^2}_{\tilde{f}_{L,R}}$. To obtain the mass eigenstates of the sfermion one has to diagonalize this matrix. This leads to two mass eigenstates of the sfermion $\{\tilde{f}_1, \tilde{f}_2\}$ and $\tilde{f}_1$ donates the lighter one.

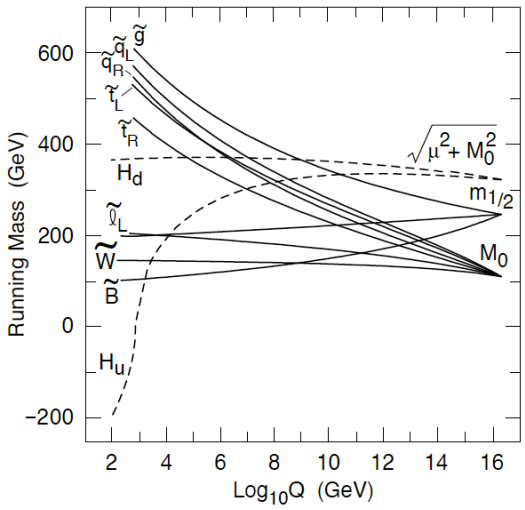

Figure 2: Energy dependence of the sparticle masses [3]

The energy dependence of the mass of the SUSY-particles can be calculated. A unification of masses at the plank scale such a dependency is shown in figure 2. There one can see that considering a uniform mass for spin 0 sparticles at a certain energy scale the mass of the stop at an energy level achievable with the LHC is lower than the masses of the other squarks.

From here on "squarks" will mean the squarks of the 1st and 2nd generation and the sbottom. For the top quark mass m_t being much larger than the masses of the other quarks and the proportionality of the off-diagonal terms to the corresponding fermion mass m_f leads, by diagonalizing the matrix of equation 2, to a lighter mass of the stop quark as of the other squarks. Due to large Yukawa coupling of the top quark the two mass eigenstates $\tilde{t}_1$ & $\tilde{t}_2$ get separated any further which leads to an even lighter stop quark mass $\tilde{t}_1$. Further on with stop quark will be meant the $\tilde{t}_1$.

An other reason for a favoured light stop quark arises by demanding a natural solution of the hierarchy problem, because a light stop quark with a mass less than one TeV would cancel out most of the loop contributions of the top quark to the Higgs divergence.

The cross-sections for different SUSY-particle production processes can be calculated depended on the masses of the sparticles. This is shown in figure 3. In this figure one can see that the cross-section of stop pair production is significantly lower than of squarks pair production assuming the same masses of the stop and the squarks. This is due to parton distribution of the colliding protons, in which there is no top quark contribution.

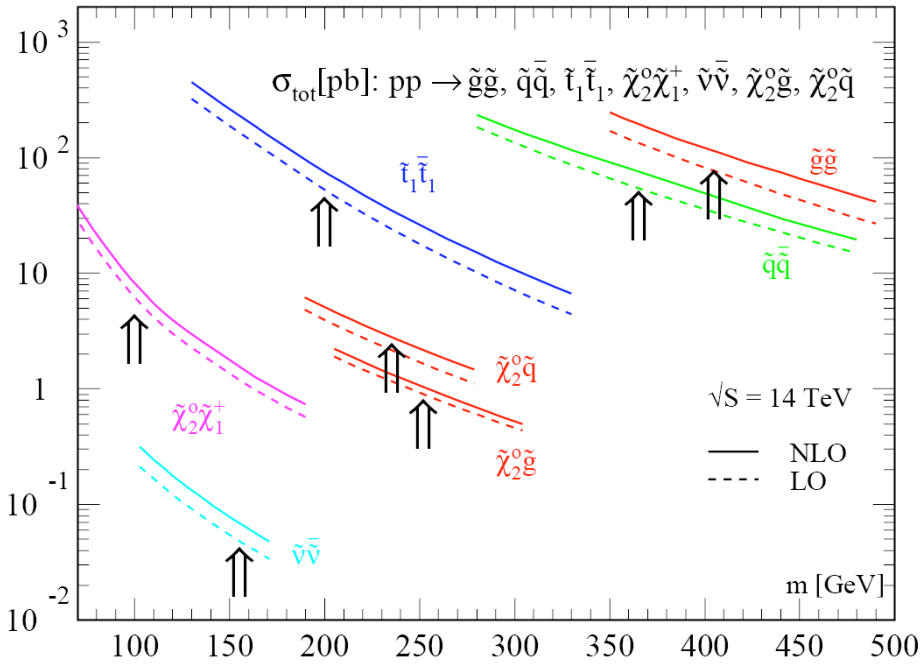

Figure 3: Cross-sections for SUSY production processes plotted against the masses of the sparticles in leading-order (LO) and next to leading-order (NLO) [3]

2.1 Considered processes

2.1.1 Considered decay modes

In the here presented searches only direct stop pair production is considered and only two decay modes for the stop quark are assumed. The first decay mode considered is the stop

decaying into a top quark and the lightest neutralino. The lightest neutralino is in those two searches considered the LSP $\tilde{\chi}_0^1$. The second is the stop quark decaying into a bottom quark and the lightest chargino $\tilde{\chi}_1^{\pm}$which will decay further into the LSP and an on- or off-shell W-boson, to be seen here:

- $\tilde{t}_1 \rightarrow t\ \tilde{\chi}_1^0$
- $\tilde{t}_1 \rightarrow b\ \tilde{\chi}_1^{\pm} \rightarrow b\ \tilde{\chi}_1^0\ W^{(*)}$

In the analysis of the two presented searches, different branching-ratios (BR) of the decay modes are considered.

2.1.2 Detector signature

The top quark arising in the decay products can decay either hadronically or leptonically and also the W-boson. This leads to four final states arising out of a single stop decay. The feynman graphs for those final states can be seen in figure 4 a and b. To get the final states from a decaying stop pair two of those feynmans have to be combined. This leads to three different final states:

- 0 leptons (all hadronic)
- 1 lepton
- 2 leptons

Two examples of Feynman-graphs of such final states can be seen in figure 4 c and d. In the first search presented here only final states with zero leptons are used and the second presented search focuses on final states with one isolated lepton.

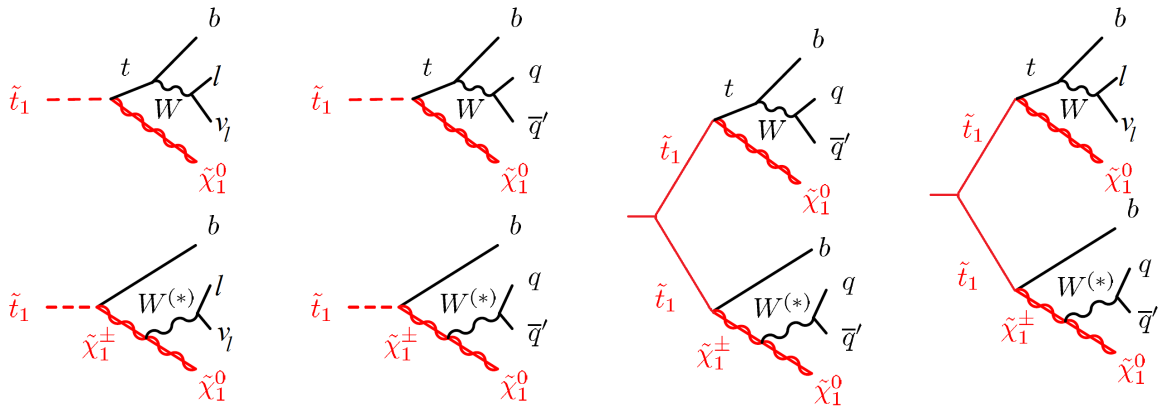

(a) (b) [4] (c) (d)

Figure 4: a & b: Feynmans for the final states arising out of a single stop decay, (a) final states with one lepton and (b) all hadronic final states; c & d: possible final states of a decaying stop pair with one lepton in the final state (c) and a full hadronic final state (d)

The signature of such final states is that there are at least four jets (for the 1 lepton case), while at least two of them are b-tagged and there is a huge amount of missing transverse energy (E_t^{miss}) due to the LSP which escapes the detector undetected. A possible stop pair production event recorded with the Atlas detector is shown in figure 5, where five jets were measured (white cones) while two of them are b-tagged (blue cones). The missing transverse energy in this event is $E_t^{miss} = 896\,\text{GeV}$.

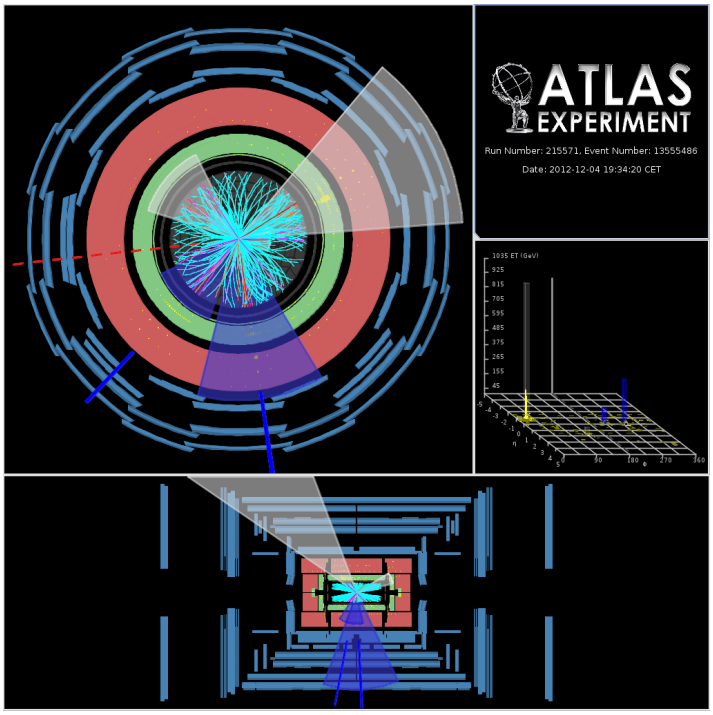

Figure 5: Possible event for stop pair production, taken in 2012 [5]

3 Search for all hadronic final states

Lets begin with the first search, the search after full hadronic final states only. This search was published in 2014 by the ATLAS Collaboration. All data, results and figures presented here are based on the source [4]. The analyzed data was taken by the ATLAS detector at the LHC and 20.1 fb^{-1} of data was used. Only events with no lepton in the final state were used.

3.1 Signal regions

To gain sensitivity to different masses of the stop and the LSP, signal regions (SR) with different selection criteria are defined. The signal regions are labled SRA1-4, SRB1-2 and SRC1-3, shown in table 1. For increasing label number stricter event selection criteria are applied on the main label criteria. For SRA the main label criteria is the missing transverse energy (E_t^{miss}), for SRB the main label criteria is the top mass asymmetry ($\mathcal{A}_{m_t}$) and for SRC it is $m_T^{b,\text{min}}$ which is the transverse mass from the E_t^{miss} and the closest b-tagged jet.

SR	main label criteria	sensitive for:
SRA1-4	E_T^{miss}	$\tilde{t}_1 \to t\,\tilde{\chi}_0^1$
SRB1-2	$\mathcal{A}_{m_t}$	$\tilde{t}_1 \to b\,\tilde{\chi}_1^{\pm}$
SRC1-3	$m_T^{b,\text{min}}$	$\tilde{t}_1 \to t\,\tilde{\chi}_0^1$

Table 1: Sensitivity of signal regions and main label criteria

The event selection criteria applied to the signal regions are as follows. All selection criteria are optimized to minimize background (BG) events. For all signal regions the selection criteria shown in table figure 6. As one can see the number of leptons N_{lep} in an event must be zero to be selected, additionally there must be at least two b-tagged jets and a missing transverse energy larger than 150 GeV. To reject events arising from mismeasured jets an angular separation $\left|\Delta\phi\left(jet, \mathbf{p}_T^{\text{miss}}\right)\right|$ between the azimuthal angle ϕ of the $E_t^{miss}$and each of the three highest jets is applied. For the same reason a requirement on $\left|\Delta\phi\left(\mathbf{p}_T^{\text{miss}}, \mathbf{p}_T^{\text{miss,track}}\right)\right|$ is set. The restriction for $m_T^{\text{b,min}}$ is set to minimize BG contributed by $t\bar{t}$-production. In figure 7 the number of events is plotted over the $m_T^{\text{b,min}}$. Here one can see that for $m_T^{\text{b,min}} < 175$ there is a large BG contribution from $t\bar{t}$-production and therefore the criteria for this parameter is set.

Trigger	$E_{\text{T}}^{\text{miss}}$
N_{lep}	0
b-tagged jets	≥ 2
$E_{\text{T}}^{\text{miss}}$	> 150 GeV
$\left\|\Delta\phi\left(\text{jet}, \mathbf{p}_{\text{T}}^{\text{miss}}\right)\right\|$	$> \pi/5$
$\left\|\Delta\phi\left(\mathbf{p}_{\text{T}}^{\text{miss}}, \mathbf{p}_{\text{T}}^{\text{miss,track}}\right)\right\|$	$< \pi/3$
$m_{\text{T}}^{b,\text{min}}$	> 175 GeV

Figure 6: Selection criteria applied to all SR

The signal regions SRA are called fully resolved for every jet being isolated and can be measured separately, therefore at least 6 jets are needed for this signal region. The selection

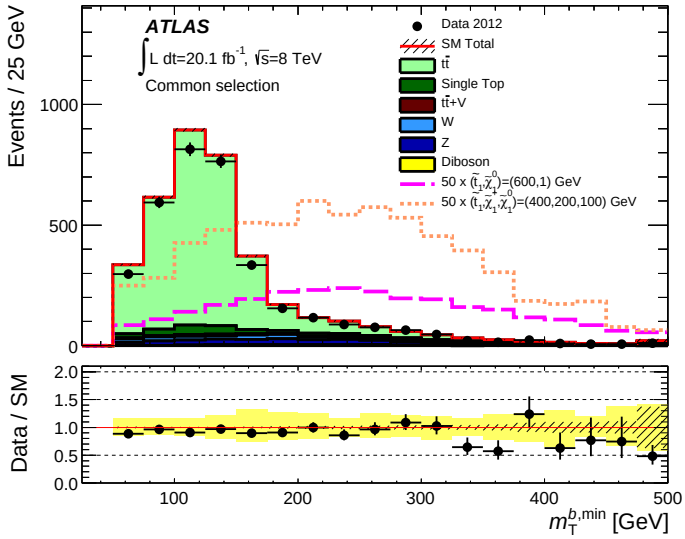

Figure 7: $m_T^{\mathrm{b,min}}$ distribution for events with at least 4 jets and all selection criteria applied except for $m_T^{\mathrm{b,min}}$

criteria are shown in figure 8. The signal regions SRB and SRC are only partially resolved needing 4-5 jets in SRB and exactly 5 jets for SRC due to a boosted top overlapping decay products. The selection criteria are shown in figure 9 for SRB and for SRC in figure 10.

	SRA1	SRA2	SRA3	SRA4
anti-k_t $R = 0.4$ jets	≥ 6, $p_{\mathrm{T}} > 80, 80, 35, 35, 35, 35$ GeV			
m^0_{bjj}	< 225 GeV		[50,250] GeV	
m^1_{bjj}	< 250 GeV		[50,400] GeV	
$\min[m_{\mathrm{T}}(\mathrm{jet}^j, \mathbf{p}_{\mathrm{T}}^{\mathrm{miss}})]$	–		> 50 GeV	
τ veto	yes			
$E_{\mathrm{T}}^{\mathrm{miss}}$	> 150 GeV	> 250 GeV	> 300 GeV	> 350 GeV

Figure 8: Event selection criteria for SRA

	SRB1	SRB2
anti-k_t $R = 0.4$ jets	4 or 5, $p_{\mathrm{T}} > 80, 80, 35, 35, (35)$ GeV	5, $p_{\mathrm{T}} > 100, 100, 35, 35, 35$ GeV
$\mathscr{A}_{m_t}$	< 0.5	> 0.5
$p^0_{\mathrm{T,jet},R=1.2}$	–	> 350 GeV
$m^0_{\mathrm{jet},R=1.2}$	> 80 GeV	[140, 500] GeV
$m^1_{\mathrm{jet},R=1.2}$	[60, 200] GeV	–
$m^0_{\mathrm{jet},R=0.8}$	> 50 GeV	[70, 300] GeV
$m_{\mathrm{T}}^{\mathrm{min}}$	> 175 GeV	> 125 GeV
$m_{\mathrm{T}}(\mathrm{jet}^3, \mathbf{p}_{\mathrm{T}}^{\mathrm{miss}})$	> 280 GeV for 4-jet case	–
$E_{\mathrm{T}}^{\mathrm{miss}}/\sqrt{H_{\mathrm{T}}}$	–	$> 17\sqrt{\mathrm{GeV}}$
$E_{\mathrm{T}}^{\mathrm{miss}}$	> 325 GeV	> 400 GeV

Figure 9: Event selection criteria for SRB

Now that the event selection criteria are defined the background has to be estimated.

	SRC1	SRC2	SRC3
anti-k_t $R = 0.4$ jets	5, $p_T > 80, 80, 35, 35, 35$ GeV		
$\lvert\Delta\phi(b,b)\rvert$	$> 0.2\pi$		
$m_T^{b,\min}$	> 185 GeV	> 200 GeV	> 200 GeV
$m_T^{b,\max}$	> 205 GeV	> 290 GeV	> 325 GeV
τ veto	yes		
E_T^{miss}	> 160 GeV	> 160 GeV	> 215 GeV

Figure 10: Event selection criteria for SRC

3.2 Background estimation

To estimate the BG it is important to know which Standard Modelprocesses can end up in the same final states as we want to detect. Therefore lets have a look on the Feynman-graphs for the stop pair production and its decay-chains, shown in figure 11a. The detector signature is at least 4 jets (for having overlapping decay products) where 2 of them are b-tagged and a high E_t^{miss}. Such final states can also be build using Standard Modelprocesses alone, seen in figure 11b&c. The Feynman-graph in the middle shows the main BG contribution from $t\bar{t}$-production decaying semileptonically, the two on the right are representing BG contribution from vector-boson production and gluon emission from the initial quarks, where the lepton for the lower case escapes the detector undetected or is mismeasured as jet. For the different signal regions different Standard Modelprocesses have to be considered as BG.

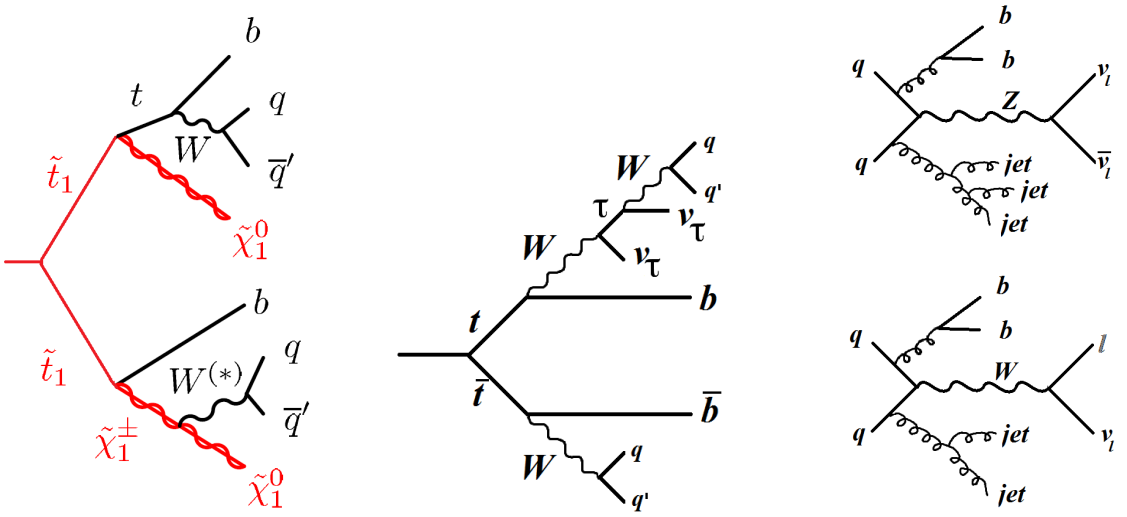

(a) (b) (c)

Figure 11: a) Feynman-graph for final states tried to detect, b) & c) Standard Model processes with the same final states we want to detect and therefore BG events

The background in the signal regions is simulated with Monte-Carlo-Simulations (MCS), but using MCS alone would lead to high uncertainties. Therefore control regions (CR) and validation regions (VR) are defined orthogonal to each other and to the signal regions. The

simulations are then normalized to the CR and transferred to the validation- and signal regions. In the validation regions it is assumed that there are no SUSY-processes. So if the transferred BG simulations are describing the number of events observed in the validation regions the used background models are good and hopefully will describe the BG in our signal regions well enough.

As an example the Z+jets CR will be discussed briefly. The event selection criteria are shown in figure 12. As it can be seen an event in this control region needs exactly 2 leptons (electrons or muons). The transverse energy and the transverse momentum of the two leptons are then threatened as E_t^{miss} and missing transverse momentum p_t^{miss}, an event is rejected if the E_t^{miss} from the two leptons is below 70 GeV. Since to this point no requirement on the number of b-tagged jets is set, the number of events has to be corrected with the $b\bar{b}$-fraction. Afterwards the MC simulations are normalized to this CR. The selection criteria for the VR of SRA are the same as for the SR except the requirements on the top mass and on the $m_T^{\mathrm{b,min}}$ were changed and also the τ-veto is inverted. The normalization and the transferring is done with a simultaneous likelihood fit in all SR,CR and VR. The BG from $t\bar{t}$-production decaying full hadronically and multijet events is estimated without MCS, but it is estimated using CR and VR alone.

	$t\bar{t}$ **CR**	Z + jets **CR**	**Multijet CR**
Trigger	electron (muon)	electron (muon)	same
N_{lep}	1	2	same
p_{T}^{ℓ}	$>35(35)$ GeV	$>25(25)$ GeV	–
$p_{\mathrm{T}}^{\ell_2}$	same	$>10(10)$ GeV	same
$m_{\ell\ell}$	–	$[86,96]$ GeV	–
$E_{\mathrm{T}}^{\mathrm{miss,track}}$	–	–	same
$\left\lvert\Delta\phi\left(\mathbf{p}_{\mathrm{T}}^{\mathrm{miss}},\mathbf{p}_{\mathrm{T}}^{\mathrm{miss,track}}\right)\right\rvert$	–	–	–
$\lvert\Delta\phi\left(\mathrm{jet},\mathbf{p}_{\mathrm{T}}^{\mathrm{miss}}\right)\rvert$	$>\pi/10$	–	<0.1
$m_{\mathrm{T}}^{b,\mathrm{min}}$	>125 GeV	–	–
$m_{\mathrm{T}}\left(\ell,\mathbf{p}_{\mathrm{T}}^{\mathrm{miss}}\right)$	$[40,120]$ GeV	–	–
$\min[m_{\mathrm{T}}\left(\mathrm{jet}^{l},\mathbf{p}_{\mathrm{T}}^{\mathrm{miss}}\right)]$	–	–	–
m_{bjj}^{0} or m_{bjj}^{1}	<600 GeV	–	–
$E_{\mathrm{T}}^{\mathrm{miss}}$	>150 GeV	<50 GeV	>150 GeV
$\left(E_{\mathrm{T}}^{\mathrm{miss}}\right)'$	–	>70 GeV	–

Figure 12: Selection criteria for the CRs of the SRA signal region

Lets compare the data in the CR and the VR to the normalized MCS, beginning with the control regions, shown in figure 13. The number of events directly obtained from the Monte-Carlo-simulations are shown under the "Expected events". As expected the observed number of events is equal to the fitted background events for normalizing them in the control regions.

	CRs for SRA			CRs for SRB				CRs for SRC		
	$t\bar{t}$	Z + jets	Multijets	$t\bar{t}$	W + jets	Z + jets	Multijets	$t\bar{t}$	Z + jets	Multijets
Observed events										
	247	101	592	950	440	499	2082	313	499	1017
Fitted background events										
Total SM	247 ± 16	101 ± 10	593 ± 27	950 ± 40	440 ± 27	499 ± 22	2082 ± 48	313 ± 18	499 ± 22	1018 ± 34
$t\bar{t}$	197 ± 21	12.6 ± 3.0	109 ± 23	800 ± 50	189 ± 25	46 ± 7	140 ± 14	239 ± 24	49 ± 12	115 ± 23
Z + jets	0.28 ± 0.19	73 ± 11	2.5 ± 0.6	0.59 ± 0.16	1.40 ± 0.25	423 ± 25	11.7 ± 1.6	0.18 ± 0.07	420 ± 26	6.7 ± 0.9
W + jets	20 ± 9	–	4.5 ± 2.2	54 ± 20	190 ± 40	–	18 ± 7	28 ± 12	–	9 ± 4
Multijets	–	–	460 ± 40	–	–	–	1890 ± 50	–	–	870 ± 40
Others	29 ± 4	15 ± 4	11.8 ± 1.6	93 ± 13	61 ± 8	30 ± 10	22.7 ± 3.0	45 ± 7	30 ± 7	12.6 ± 1.6
Expected events (before fit)										
$t\bar{t}$	159	10.2	88	800	190	46	140	224	46	108
Z + jets	0.31	78	2.7	0.55	1.30	394	10.9	0.17	394	6.3
W + jets	20	–	4.5	52	180	–	17	28	–	9
Multijets	–	–	460	–	–	–	2090	–	–	870
Others	29	15	11.7	93	61	30	22.7	45	30	12.6

Figure 13: Observed data and MCS before and after normalization

The most interesting regions are the validation regions, they are important to check if the BG is known well enough. The expected BG and the number of events in the VR are shown in figure 14. It can be seen that the used BG models describe the observed data in the range of 2 standard deviations.

	VRA1	VRA2	VRB	VRC1	VRC2
Observed events					
	158	51	69	103	24
Fitted background events					
Total SM	189 ± 26	50 ± 6	70 ± 19	110 ± 12	21.1 ± 2.9
$t\bar{t}$	170 ± 27	34 ± 7	60 ± 19	93 ± 12	17.3 ± 2.8
Z + jets	4.0 ± 1.1	1.5 ± 0.4	1.5 ± 0.5	6.9 ± 1.5	0.24 ± 0.20
W + jets	2.8 ± 1.2	4.8 ± 2.2	2.1 ± 1.4	3.9 ± 1.8	1.1 ± 0.5
Others	11.8 ± 3.1	9.1 ± 2.2	7.2 ± 2.5	6.7 ± 2.0	2.4 ± 0.7

Figure 14: Normalized BG simulations and data in the VR

3.3 Results

Now that the BG is described quiet well, one can have a look on the signal regions. Beginning with some E_t^{miss}-distributions for the signal regions SRA, shown in figure 15. The data shown is well described by the BG models alone and no significant deviation is observed. Additionally there are expected distributions shown for a stop mass of 600 GeV and a light LSP with a mass of 1 GeV, but those distributions are not describing the observed data. The same can be seen for the other signal regions SRB and SRC, the distributions are shown in the attachment. In all distributions it can be seen that the number of events is very small.

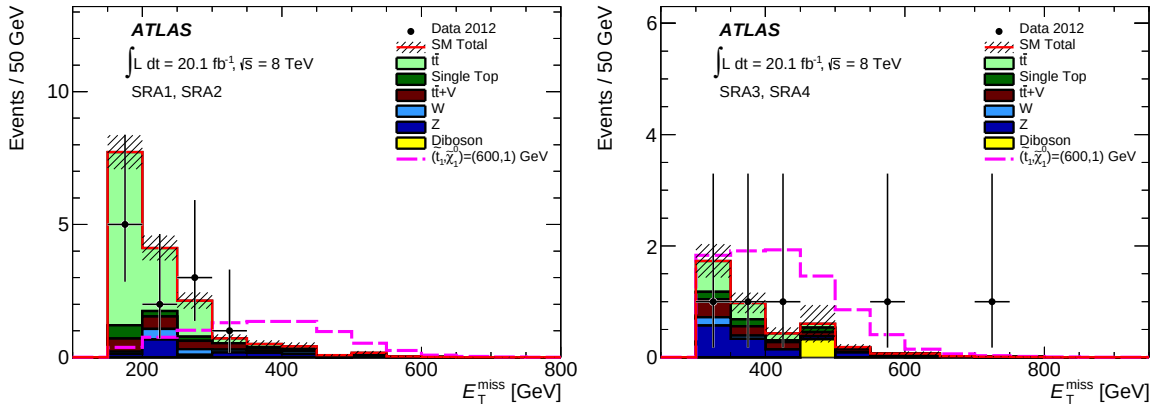

(a) (b)

Figure 15: E_t^{miss}-distributions for the signal region SRA, the distributions for the signal regions SRB and SRC are in the appendix

Lets have a look at the number of events observed and expected in each signal region. The corresponding table is shown in figure 16. In this table the same conclusion can be made as for the E_t^{miss}-distributions, no significant deviation between Standard Modelexpectation and observed data is seen. From the expected number of events and from observed data one can derive the expected and observed visible cross-section limits $\sigma_{\text{vis}}(exp)$& $\sigma_{\text{vis}}(obs)$.

From the number of events (observed or expected) all cross-sections can be excluded which would lead to a larger number of events. The highest cross-section for a given confidence level (CL) is then obtained by shifting the probability distribution for the searched cross-section as much to the left that the area confined with the median of the BG estimation ($\sigma_{\text{vis}}(exp)$) or with the number of observed events ($\sigma_{\text{vis}}(obs)$) and the probability distribution is about 100%−CL. The common CL is 95%.

The measured $\sigma_{\text{vis}}(exp)$ and $\sigma_{\text{vis}}(obs)$from the table in figure 16 are equal in the range of 2 σ. The expected and observed visible cross-section are universal results. Applying models one can derive exclusion regions for sparticle masses out of those cross-section limits. This procedure can be seen in figure 18, this figure does not belong to this search, but it illustrates the approach done here. The blue lines correspond to the theoretical cross-section calculated depending on the stop masses. The yellow and red distributions are the observed and expected

	SRA1	SRA2	SRA3	SRA4	SRB	SRC1	SRC2	SRC3
Observed events	11	4	5	4	2	59	30	15
Total SM	15.8 ± 1.9	4.1 ± 0.8	4.1 ± 0.9	2.4 ± 0.7	2.4 ± 0.7	68 ± 7	34 ± 5	20.3 ± 3.0
$t\bar{t}$	10.6 ± 1.9	1.8 ± 0.5	1.1 ± 0.6	0.49 ± 0.34	$0.10^{+0.14}_{-0.10}$	32 ± 4	12.9 ± 2.0	6.7 ± 1.2
$t\bar{t}+W/Z$	1.8 ± 0.6	0.85 ± 0.29	0.82 ± 0.29	0.50 ± 0.17	0.47 ± 0.17	3.2 ± 0.8	1.9 ± 0.5	1.3 ± 0.4
Z + jets	1.4 ± 0.5	0.63 ± 0.22	1.2 ± 0.4	0.68 ± 0.27	1.23 ± 0.31	15.7 ± 3.5	9.0 ± 1.9	6.1 ± 1.3
W + jets	1.0 ± 0.5	0.46 ± 0.21	0.21 ± 0.19	$0.06^{+0.10}_{-0.06}$	0.49 ± 0.33	8 ± 4	4.8 ± 2.2	2.8 ± 1.2
Single top	1.0 ± 0.4	0.30 ± 0.17	0.44 ± 0.14	0.31 ± 0.16	0.08 ± 0.06	7.2 ± 2.9	4.5 ± 1.8	2.9 ± 1.4
Diboson	< 0.4	< 0.13	0.32 ± 0.17	0.32 ± 0.18	0.02 ± 0.01	1.1 ± 0.8	$0.6^{+0.7}_{-0.6}$	$0.6^{+0.7}_{-0.6}$
Multijets	< 0.001	< 0.001	< 0.001	< 0.001	< 0.001	0.24 ± 0.24	0.06 ± 0.06	0.01 ± 0.01
σ_{vis} (obs) [fb]	0.33	0.29	0.33	0.32	0.21	0.78	0.62	0.40
σ_{vis} (exp) [fb]	$0.48^{+0.21}_{-0.14}$	$0.29^{+0.13}_{-0.09}$	$0.29^{+0.14}_{-0.09}$	$0.25^{+0.13}_{-0.07}$	$0.24^{+0.13}_{-0.06}$	$1.03^{+0.42}_{-0.29}$	$0.73^{+0.31}_{-0.21}$	$0.55^{+0.24}_{-0.15}$
N^{95}_{obs}	6.6	5.7	6.7	6.5	4.2	15.7	12.4	8.0
N^{95}_{exp}	$9.7^{+4.3}_{-3.0}$	$5.8^{+2.6}_{-1.8}$	$5.9^{+2.8}_{-1.9}$	$5.0^{+2.6}_{-1.4}$	$4.7^{+2.6}_{-1.2}$	$20.7^{+8.4}_{-5.8}$	$14.7^{+6.2}_{-4.2}$	$11.0^{+4.9}_{-3.1}$

Figure 16: Observed data, BG estimations and calculated expected/observed visible cross-section for each signal region

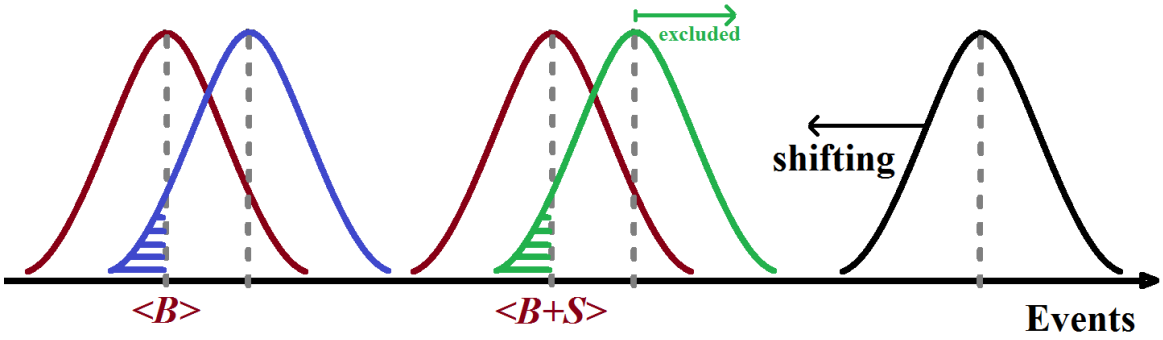

Figure 17: Very simplified schematic illustration of obtaining the expected and the visible cross-section

visible cross-section limits. Now all masses can be excluded where the visible cross-section is below the theoretical one. For simplification assumptions are made, like considering only the $\tilde{t}_1 \to t\,\tilde{\chi}^1_0$ decay and a LSP mass of $m_{\tilde{\chi}^1_0} = 50\,GeV$.

Using this proceeding one can exclude mass regions for the stop mass and the LSP mass. Such exclusion contour plots are shown in figure 19. The gray diagonal lines represent limits corresponding to the considered decay process, on these lines the initial particles and the decay products have the same masses and therefore the decay process is strongly suppressed and not possible. The gray area in figure 19 b corresponds to the LEP limit of the lightest chargino mass $m_{\tilde{\chi}^\pm_1} > 103.5\,GeV$. In these plots one can see that for a light LSP $m_{\tilde{\chi}^1_0} < 50GeV$ the stop mass must be at least about $600\,GeV$ and that the expected and observed limit are almost the same. But as to be seen the excluded regions from 2011 could be extended.

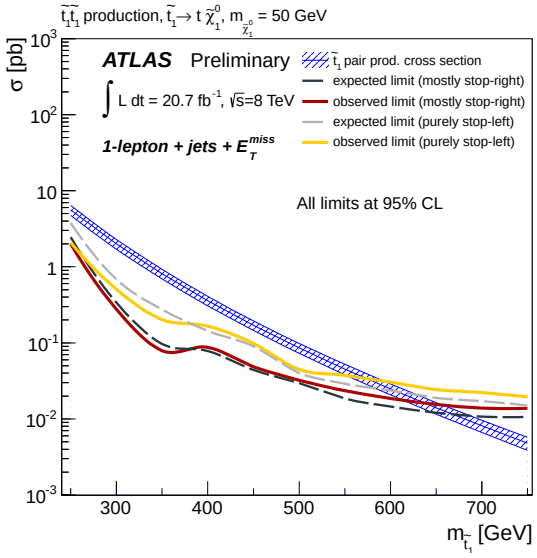

Figure 18: Calculated cross-sections for stop pair production in dependence of the stop mass. This plot does not belong to this search, but it illustrates the approach done here. [6]

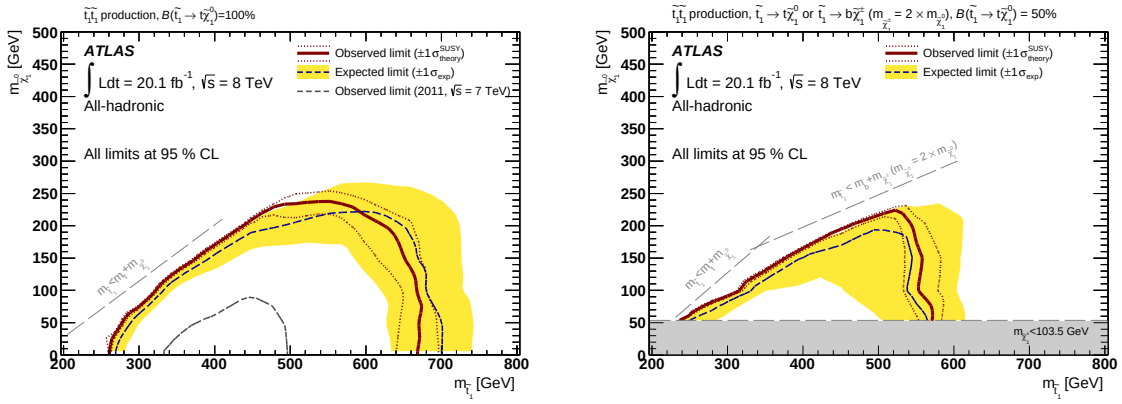

(a) (b)

Figure 19: Exclusion contour plots for different assumptions

Lets summarize the results of this search:

- BG models describes our BG from validation regions very good
- No deviation between estimated BG and observed data in signal regions
- Existing exclusion contours could be extended

4 Search for final states with one lepton

The second search presented here is the search after direct stop pair production decaying into final states with exactly one lepton. This search was done in 2013 by the ATLAS Collaboration using $20.7\,fb^{-1}$ of data taken with the ATLAS detector at the LHC with a center of mass energy of $\sqrt{s} = 8\,TeV$. All data, results and figures presented here are based on the source [6].

The basics of this search are analogue to the first presented search, therefore it won't be this detailed.

4.1 Signal regions

To gain greater sensitivity for different mass ranges and decay modes six signal regions are defined. Three of them are sensitive for the decay $\tilde{t}_1 \to b\,\tilde{\chi}_1^{\pm}$ and are labelled SRbC1-3 and the others are labelled SRtN for being sensitive for the $\tilde{t}_1 \to t\,\tilde{\chi}_0^1$ decay. In table 2 it is shown to which mass ranges the particular SR is sensitive.

SR	sensitive to:
SRbC1	$m_{\tilde{\chi}_1^{\pm}} = 100 - 300\,GeV$ & $m_{\tilde{t}_1} = 200 - 400\,GeV$
SRbC2	$m_{\tilde{t}_1} = 310 - 500\,GeV$
SRbC3	$\left(m_{\tilde{t}_1} - m_{\tilde{\chi}_1^{\pm}}\right) > 150\,GeV$
SRtN1	$m_{\tilde{t}_1} > m_t + m_{\tilde{\chi}_0^1}$
SRtN2	large $m_{\tilde{\chi}_0^1}$
SRtN3	large $m_{\tilde{t}_1}$

Table 2: Different sensitivity shown for the SR

For the SR different event selection criteria are applied, shown in figure 20. Like in the first search, the selection criteria are optimized to reduce background events. The signal region SRtN1 is spanned by the requirements on E_t^{miss} and m_T to gain higher sensitivity to the parameter space where the stop and its decay products are almost mass degenerated. As one can see in this search the criteria on the number of b-tagged jets is not always as strict as in the first search. What is not mentioned in this table is that only events with exactly one isolated lepton are considered.

4.2 Background estimation

Since now the event selection criteria are known one has to estimate the background for the different signal regions. Therefore lets have a look at some Feynman-graphs for the real final states we want to observe and at some Standard Modelprocesses having similar final states, shown in figure 21. The Feynman-graph on the left shows one decay corresponding to direct stop pair production leading to an one lepton final state. The detector signature for this process is one isolated lepton, two b-tagged jets and huge E_t^{miss}arising for the undetected LSP and the undetected neutrino. The same final states can be constructed using Standard Modelprocesses alone and have to be considered as background processes. The Feynmans for such processes are shown in figure 21b&c. The main BG contribution is from $t\bar{t}$-production decaying semileptonically and for this reason having E_t^{miss} from neutrinos. But also BG arises from Z+jets (with one lepton being undetected as such) and W+jets production.

Requirement	SRtN1_shape	SRtN2	SRtN3	SRbC1	SRbC2	SRbC3
$\Delta\varphi(\text{jet}_1, \vec{p}_{\text{T}}^{\text{miss}})$ >	0.8	-	0.8	0.8	0.8	0.8
$\Delta\varphi(\text{jet}_2, \vec{p}_{\text{T}}^{\text{miss}})$ >	0.8	0.8	0.8	0.8	0.8	0.8
$E_{\text{T}}^{\text{miss}}$ [GeV] >	$100^{(\star)}$	200	275	150	160	160
$E_{\text{T}}^{\text{miss}} / \sqrt{H_{\text{T}}}$ [GeV$^{1/2}$] >	5	13	11	7	8	8
m_{T} [GeV] >	$60^{(\star)}$	140	200	120	120	120
m_{eff} [GeV] >	-	-	-	-	550	700
am_{T2} [GeV] >	-	170	175	-	175	200
m_{T2}^{τ} [GeV] >	-	-	80	-	-	-
m_{jjj}	Yes	Yes	Yes	-	-	-
$N^{\text{iso-trk}} = 0$	-	-	-	Yes	Yes	Yes
Number of b-jets ≥	1	1	1	1	2	2
p_{T} (leading b-jet) [GeV] >	25	25	25	25	100	120
p_{T} (second b-jet) [GeV] >	-	-	-	-	50	90

Figure 20: Event selection criteria for the six SR

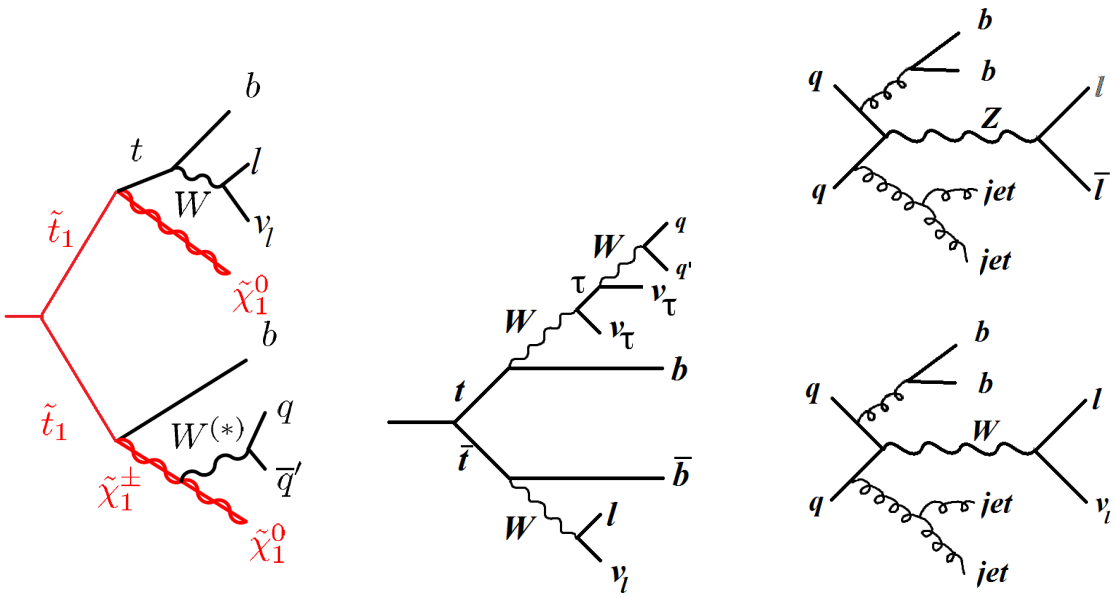

(a) (b) (c)

Figure 21: a) Feynman-graph for final states we want to detect, b) & c) Standard Modelprocesses with the same final states we want to detect and therefore BG events

The background estimation is almost the same as in the first search. The number of BG events is evaluated using MCS. Like in the first search CR and VR are defined. To minimize the uncertainties of the estimated BG the simulations were normalized to the CR and transferred to the VR and SR using a simultaneous likelihood-fit.

4.3 Results

Now that the background is estimated one can have a look onto the VR and the SR, beginning with some E_t^{miss}- or M_T-distributions for the signal regions, shown in figure 22.

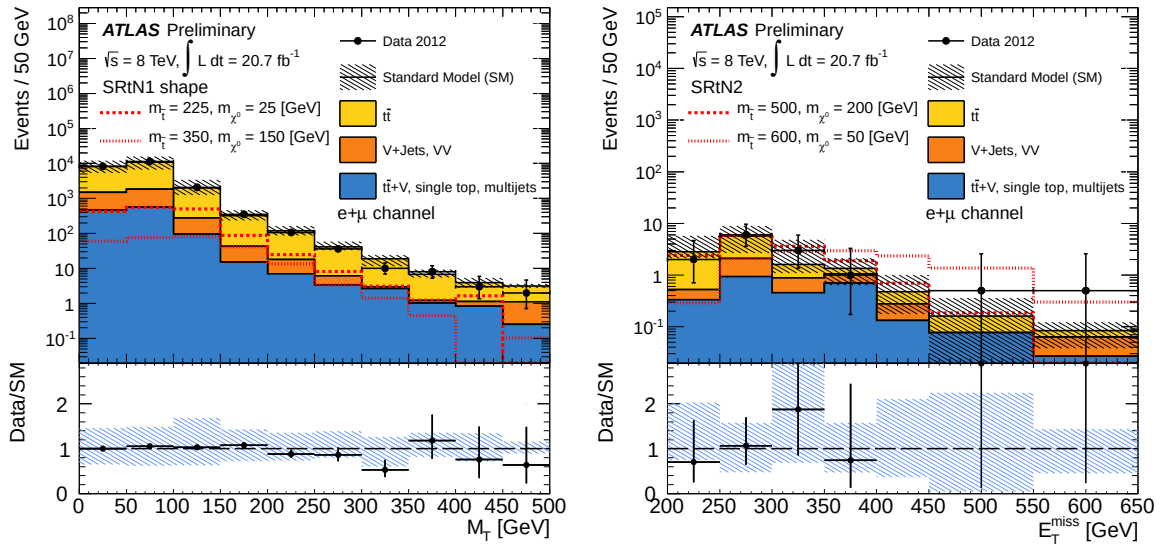

(a) (b)

Figure 22: Characteristic E_t^{miss}- or M_T-distributions for the SR: SRtN1 (a) and SRtN2 (b), the distributions for the other SR are shown in the attachment in figure 30

In all those distributions one can see that the observed data is well described by the background model alone. The red dashed lines indicates the theoretical expected distribution for different stop, chargino and LSP masses. These distributions differ significantly from the observed data. In those plots it can be seen that in comparison to the first search the number of events is quiet large.

Lets have a look at the tables containing the total number of events in each CR, VR and SR. For the signal regions SRbC it is shown in figure 23 and for the SRtN in figure 24 and 25. In the red marked areas there is the number of the observed events and the total number of estimated BG events. Since the CR are used to normalize the MCS the number of observed events must be equal to the total background, if not it would indicate that the fit went wrong. Since this is fulfilled the VR are viewed. If the number of observed events would significantly differ from the total number of estimated background events the used background model would be bad. But as one can see those numbers of events doesn't differ significantly and therefore one says that the background model is well known. Then one can compare the total BG and the number of observed events in the SR and one can see in the tables that those two numbers are equal in the range of 2σ.

Regions	WCR-SRbC1	TCR-SRbC1	TVR-SRbC1	SRbC1
Observed events	2358	2944	785	456
Total background (fit)	2358 ± 151	2944 ± 119	806 ± 123	482 ± 76
$t\bar{t}$	440 ± 180 (440)	2160 ± 210 (2170)	630 ± 100 (630)	400 ± 90 (400)
$t\bar{t}+V$	2.8 ± 1.6	14 ± 8	5.9 ± 3.4	14 ± 7
W+jets	1780 ± 240 (2080)	540 ± 170 (630)	120 ± 40 (140)	45 ± 17 (52)
Z+jets, VV, multijet	100 ± 80	37 ± 28	5 ± 5	5 ± 4
Single top	39 ± 25	190 ± 90	46 ± 31	19 ± 10
Regions	WCR-SRbC2	TCR-SRbC2	TVR-SRbC2	SRbC2
Observed events	1139	264	76	25
Total background (fit)	1139 ± 45	264 ± 19	75 ± 26	18 ± 5
$t\bar{t}$	130 ± 80 (150)	204 ± 29 (240)	61 ± 25 (71)	9 ± 5 (11)
$t\bar{t}+V$	1.3 ± 0.9	2.5 ± 1.5	1.0 ± 0.7	2.4 ± 1.3
W+jets	940 ± 100 (1000)	26 ± 12 (28)	5.8 ± 2.7 (6.2)	3.3 ± 2.0 (3.4)
Z+jets, VV, multijet	50 ± 40	1.3 ± 1.2	0 ± 0	0 ± 0
Single top	16 ± 13	30 ± 14	7 ± 5	3.4 ± 1.5
Regions	WCR-SRbC3	TCR-SRbC3	TVR-SRbC3	SRbC3
Observed events	665	144	39	6
Total background	665 ± 33	144 ± 17	42 ± 9	7 ± 3
$t\bar{t}$	60 ± 40 (80)	106 ± 23 (141)	31 ± 8 (42)	2.4 ± 1.5 (3.1)
$t\bar{t}+V$	0.8 ± 0.6	1.8 ± 1.1	0.6 ± 0.5	0.8 ± 0.6
W+jets	560 ± 60 (610)	17 ± 8 (19)	4.7 ± 2.0 (5.2)	1.7 ± 1.7 (1.9)
Z+jets, VV, multijet	33 ± 26	$0.5^{+1.2}_{-0.5}$	0 ± 0	0 ± 0
Single top	10 ± 7	18 ± 9	6 ± 4	2.0 ± 1.0

Figure 23: Table of events measured in the CR, VR and SR (for SRbC)

Regions	WCR-SRtN2	TCR-SRtN2	TVR-SRtN2	SRtN2
Observed events	165	204	23	14
Total background (fit)	165 ± 15	204 ± 16	29 ± 10	13 ± 3
$t\bar{t}$	31 ± 18 (30)	139 ± 26 (138)	22 ± 8 (22)	7.5 ± 2.9 (7.5)
$t\bar{t}+V$	0.4 ± 0.3	1.4 ± 0.8	0.4 ± 0.3	2.2 ± 1.2
W+jets	122 ± 28 (157)	44 ± 19 (57)	4.6 ± 2.6 (5.9)	1.5 ± 0.8 (1.9)
Z+jets, VV, multijet	11 ± 9	5 ± 4	$0.1^{+0.3}_{-0.1}$	0.4 ± 0.3
Single top	$1.3^{+2.4}_{-1.3}$	14 ± 10	2.1 ± 1.9	1.1 ± 0.5
Regions	WCR-SRtN3	TCR-SRtN3	TVR-SRtN3	SRtN3
Observed events	149	175	22	7
Total background (fit)	149 ± 25	175 ± 19	28 ± 14	5 ± 2
$t\bar{t}$	20 ± 15 (24)	96 ± 33 (118)	19 ± 12 (24)	1.8 ± 1.0 (2.2)
$t\bar{t}+V$	0.3 ± 0.3	1.5 ± 0.9	0.48 ± 0.35	1.0 ± 0.7
W+jets	117 ± 29 (131)	55 ± 25 (61)	5.3 ± 2.6 (5.9)	1.5 ± 1.3 (1.6)
Z+jets, VV, multijet	10 ± 8	3.8 ± 3.5	$0.1^{+0.6}_{-0.1}$	$0.14^{+0.19}_{-0.14}$
Single top	$1.6^{+1.8}_{-1.6}$	19 ± 11	2.6 ± 1.9	0.53 ± 0.24

Figure 24: Table of events measured in the CR, VR and SR (for SRtN2-3)

	= 0b-jet	≥ 1b-jet			
$100 < E_{\mathrm{T}}^{\mathrm{miss}} < 125$ GeV	$60 < m_{\mathrm{T}} < 90$ GeV	$60 < m_{\mathrm{T}} < 90$ GeV	$90 < m_{\mathrm{T}} < 120$ GeV	$120 < m_{\mathrm{T}} < 140$ GeV	$m_{\mathrm{T}} > 140$ GeV
Observed events	1289	3122	1521	268	253
Total background (fit)	1289 ± 85	3122 ± 116	1535 ± 260	291 ± 61	250 ± 57
$t\bar{t}$	480 ± 140 (430)	2720 ± 170 (2410)	1350 ± 249 (1200)	260 ± 60 (230)	230 ± 50 (200)
$t\bar{t}+V$	2.0 ± 1.0	9 ± 4	5.6 ± 2.8	1.9 ± 0.9	2.8 ± 1.3
W+jets	730 ± 170 (880)	230 ± 120 (270)	110 ± 50 (130)	22 ± 11 (26)	12 ± 10 (14)
Z+jets, VV, multijet	39 ± 35	35 ± 35	7 ± 6	$1.4^{+2.3}_{-1.4}$	$0.6^{+0.9}_{-0.6}$
Single top	31 ± 18	130 ± 70	60 ± 40	8 ± 6	6 ± 4
$125 < E_{\mathrm{T}}^{\mathrm{miss}} < 150$ GeV	$60 < m_{\mathrm{T}} < 90$ GeV	$60 < m_{\mathrm{T}} < 90$ GeV	$90 < m_{\mathrm{T}} < 120$ GeV	$120 < m_{\mathrm{T}} < 140$ GeV	$m_{\mathrm{T}} > 140$ GeV
Observed events	825	1962	721	119	165
Total background (fit)	825 ± 56	1962 ± 60	755 ± 119	145 ± 23	174 ± 28
$t\bar{t}$	330 ± 120 (290)	1740 ± 100 (1510)	670 ± 110 (590)	135 ± 21 (118)	162 ± 27 (141)
$t\bar{t}+V$	1.4 ± 0.9	7.0 ± 3.5	3.9 ± 2.2	1.3 ± 0.7	2.9 ± 1.3
W+jets	450 ± 130 (640)	130 ± 60 (180)	47 ± 25 (68)	5 ± 5 (7)	3^{+5}_{-3} (5)
Z+jets, VV, multijet	30 ± 24	16^{+27}_{-16}	3.4 ± 3.4	0.4 ± 0.4	$0.8^{+1.0}_{-0.8}$
Single top	19 ± 12	78 ± 35	27 ± 19	$3.4^{+3.5}_{-3.4}$	5.7 ± 1.9
$E_{\mathrm{T}}^{\mathrm{miss}} > 150$ GeV	$60 < m_{\mathrm{T}} < 90$ GeV	$60 < m_{\mathrm{T}} < 90$ GeV	$90 < m_{\mathrm{T}} < 120$ GeV	$120 < m_{\mathrm{T}} < 140$ GeV	$m_{\mathrm{T}} > 140$ GeV
Observed events	1441	2591	663	113	235
Total background (fit)	1441 ± 103	2591 ± 104	695 ± 151	101 ± 26	262 ± 34
$t\bar{t}$	430 ± 180 (420)	2100 ± 180 (2030)	590 ± 120 (570)	88 ± 23 (85)	220 ± 40 (210)
$t\bar{t}+V$	2.7 ± 1.7	14 ± 8	5.7 ± 3.5	2.2 ± 1.2	10 ± 5
W+jets	920 ± 210 (1110)	310 ± 120 (380)	59 ± 28 (72)	6.0 ± 3.5 (7.3)	24 ± 14 (29)
Z+jets, VV, multijet	60 ± 60	24 ± 22	2^{+5}_{-2}	$0.4^{+0.6}_{-0.4}$	2.1 ± 1.8
Single top	27 ± 20	140 ± 80	37 ± 26	4 ± 4	7 ± 5

Figure 25: Table of events measured in the CR, VR and SR (for SRtN1)

From this point one can calculate the expected and observed visible cross-sections and compute exclusion contour plots analogically to the first search. The corresponding plots are shown in figure 26. The gray diagonal lines are analogue to those in the first search. In those plots one can see that most likely the same areas are excluded as in the first search. Exclusion limits are also shown from earlier searches and as one can see those limits could be enlarged.

Lets summarize the results of this search:

- BG models describes our estimated BG in validation regions quiet good
- No deviation between estimated BG and observed data
- Exclusion contours could be extended

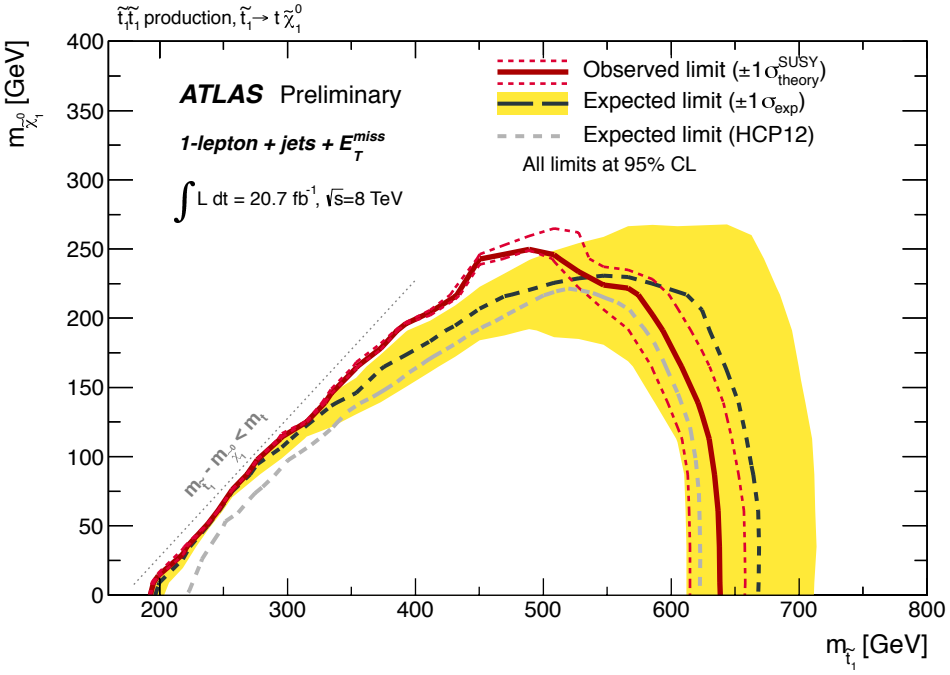

(a)

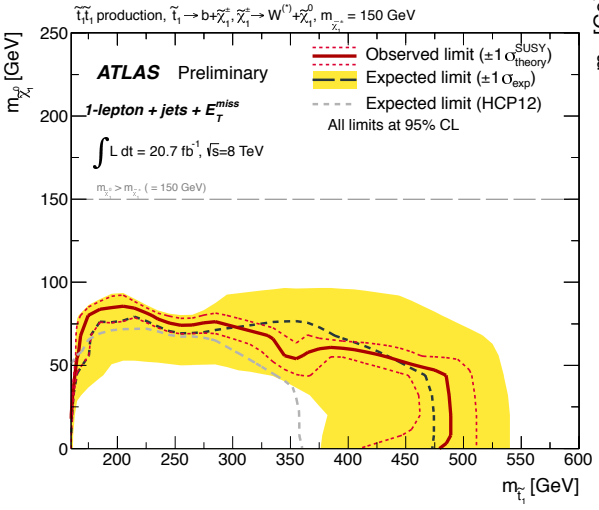

(b)

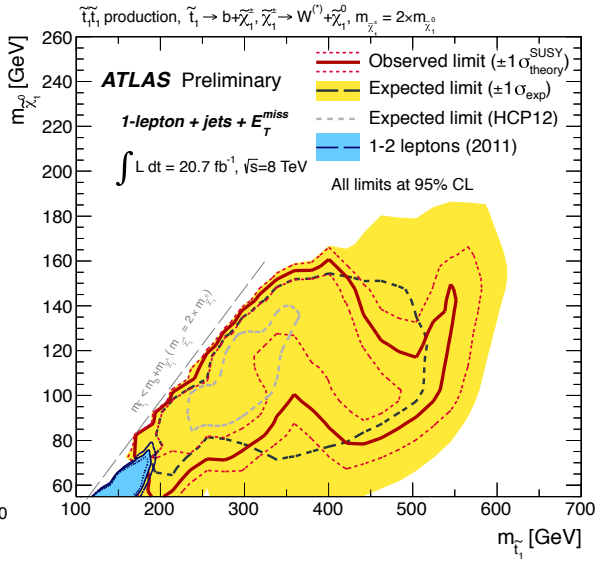

(c)

Figure 26: Exclusion contour plots for different assumptions of the branching-ratios and sparticle masses. Assumptions: direct stop pair production, (a) $BR\left(\tilde{t}_1 \to t\,\tilde{\chi}_0^1\right) = 100\%$, (b) $BR\left(\tilde{t}_1 \to b\,\tilde{\chi}_1^\pm\right) = 100\%\&m_{\tilde{\chi}_1^\pm} = 2 \cdot m_{\tilde{\chi}_0^1}$, (c) $BR\left(\tilde{t}_1 \to b\,\tilde{\chi}_1^\pm\right) = 100\%\&m_{\tilde{\chi}_1^\pm} = 150\,GeV$

5 State of the art

The two presented searches are not the only searches for SUSY-production processes. Even for direct stop pair production there are several searches, like some for final state with two leptons. In other searches different exclusion contours can be obtained by assuming different BR of the considered decay modes and assuming different sparticle masses.

In all the searches done so far no evidence for physics beyond the Standard Modelis seen. But exclusion regions in the plane spanned by two sparticle masses could be calculated.

5.1 ATLAS

The state of the art of the exclusion contours in the stop-LSP-mass plane from the ATLAS Experiment is shown in figure 27. Here one can see that for searches after different final states and while applying different assumptions, different regions can be excluded.

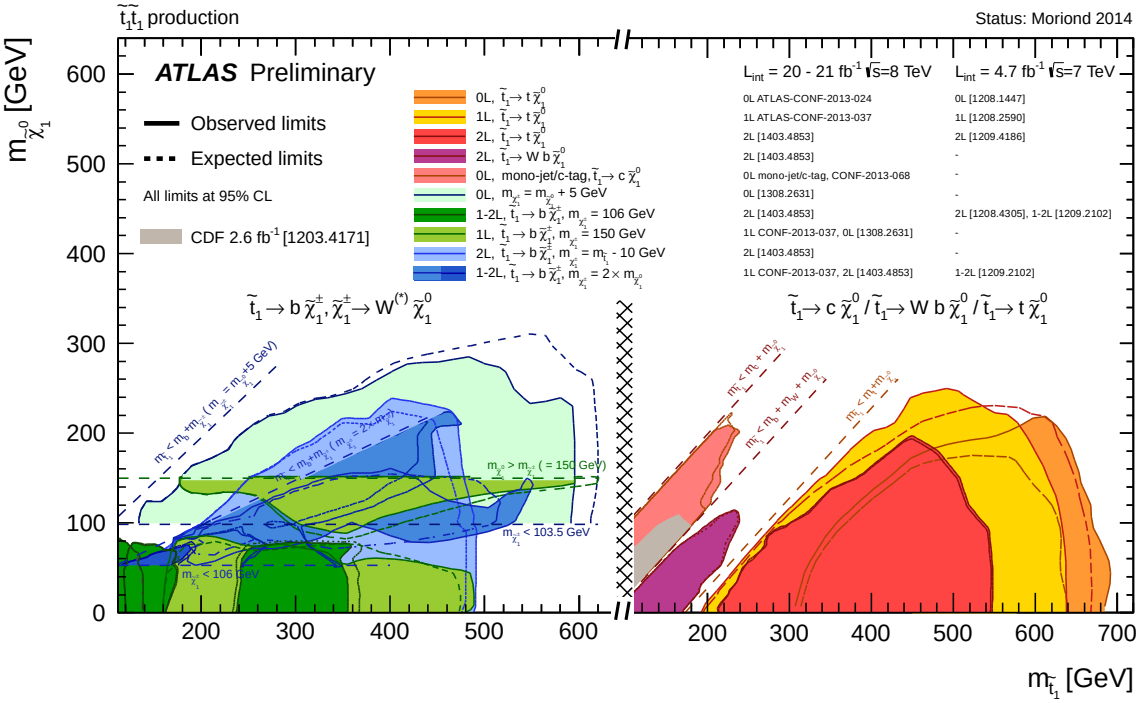

Figure 27: Combined results for the exclusion limits in the stop-LSP-mass plane for the ATLAS Experiment [7]

5.2 CMS

The CMS Experiment had also done searches after SUSY-particles production and their state of the art of exclusion limits in the stop-LSP-mass plane is shown in figure 28. What can be seen here is that the results of the CMS Experiment and the ATLAS Experiment are nearly the same.

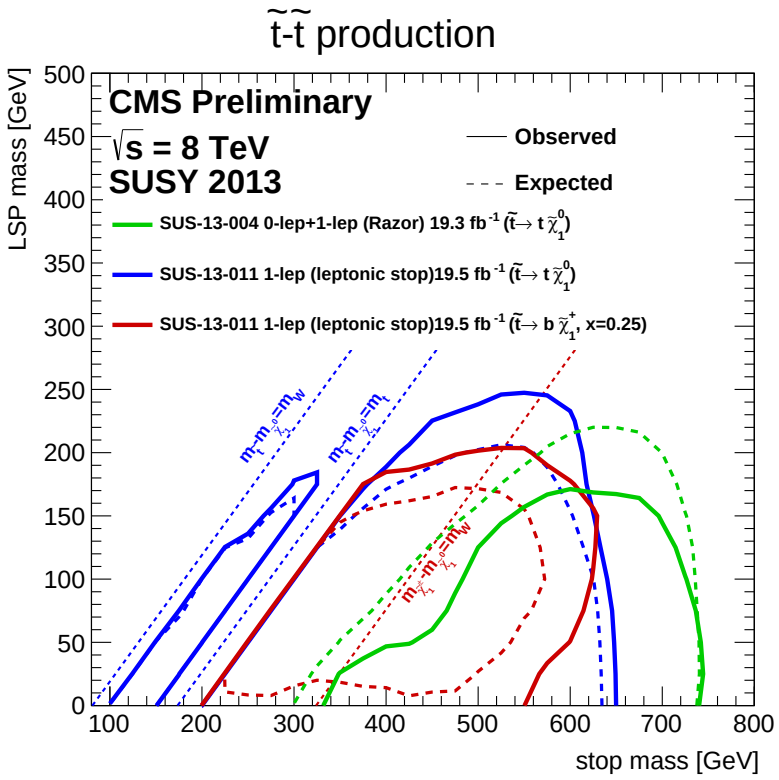

Figure 28: Combined results for the exclusion limits in the stop-LSP-mass plane for the CMS Experiment [8]

5.3 Summarization

Two searches after direct stop pair production were presented in chapter 3 & 4. The background models described the number of observed events in the validation regions very good what suggests that the background in the used signal regions is also well known. There was no significant deviation between the observed data in the signal regions and the estimated background. From the expected and the observed visible cross-sections of the data exclusion contour limits are calculated and the previous ones could be extended.

The results of the two searches are in accordance with the results of the other searches done for sparticle production. In all collider experiments so far there is no evidence for *Supersymmetry*-particle production. But from the results mass regions for the sparticles masses could be excluded. In both experiments there is no evidence for *Supersymmetry* particles and also the excluded mass regions are alike.

References

[1] Jonathan Richard Ellis. Beyond the Standard Model for Hillwalkers. (hep-ph/9812235. CERN-TH-98-329):64 p, Dec 1998.

[2] Mirjam Fehling-Kaschek. Search for scalar bottom and top quarks with the atlas detector at the lhc.

[3] Prof. Karl Jakobs. Searches for physics beyond the standard model at the lhc.

[4] Georges Aad et al. Search for direct pair production of the top squark in all-hadronic final states in proton-proton collisions at $\sqrt{s} = 8$ TeV with the ATLAS detector. 2014.

[5] ATLAS Collaboration. Search for direct pair production of the top squark in all-hadronic final states in proton-proton collisions at sqrt(s) = 8 tev with the atlas detector.

[6] Search for direct top squark pair production in final states with one isolated lepton, jets, and missing transverse momentum in $sqrts = 8$,TeV pp collisions using 21 fb^{-1} of ATLAS data. Technical Report ATLAS-CONF-2013-037, CERN, Geneva, Mar 2013.

[7] Collaboration ATLAS. Summary plots from the atlas supersymmetry physics group.

[8] Keith Ulmer. Summary of comparison plots in simplified models spectra for the 8tev dataset.

6 Appendix

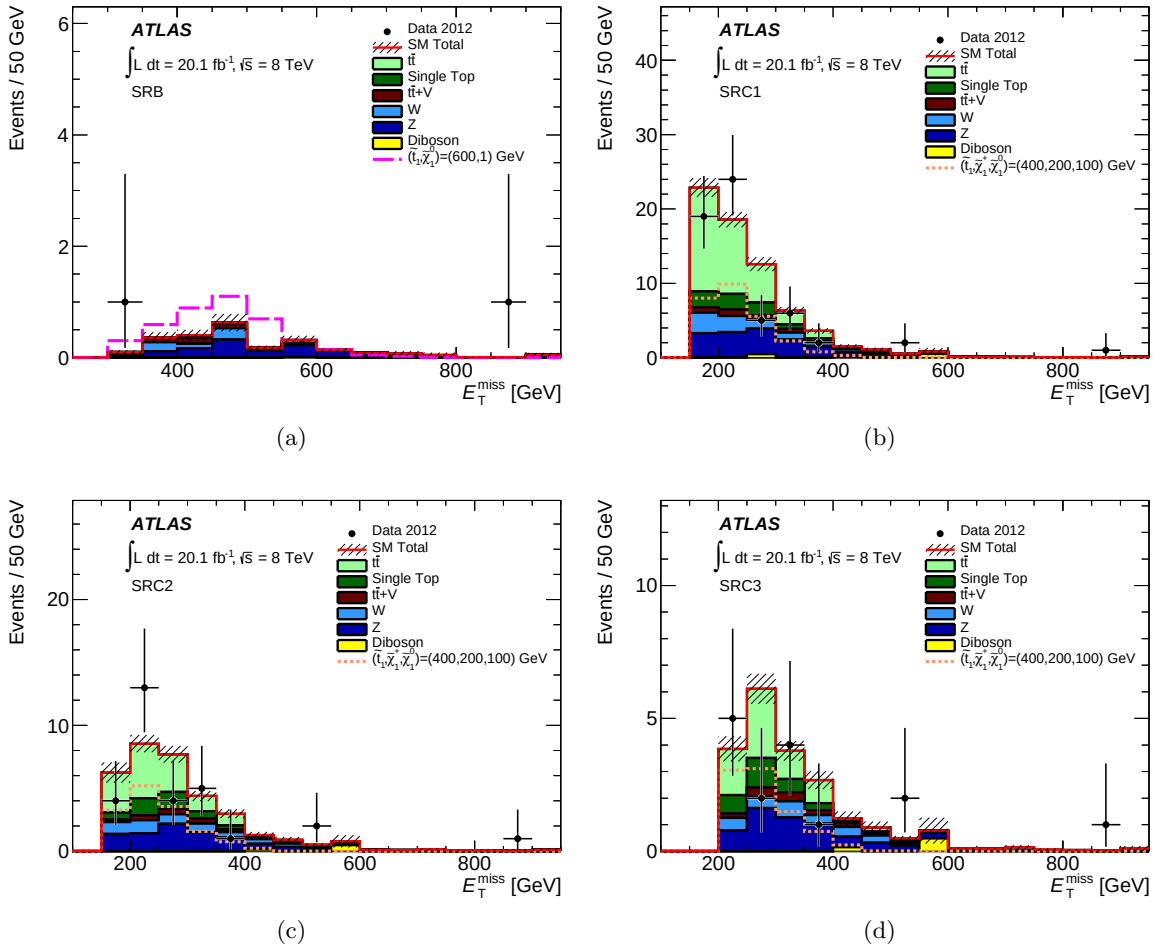

Figure 29: E_t^{miss}-distributions for the signal region SRB and SRC

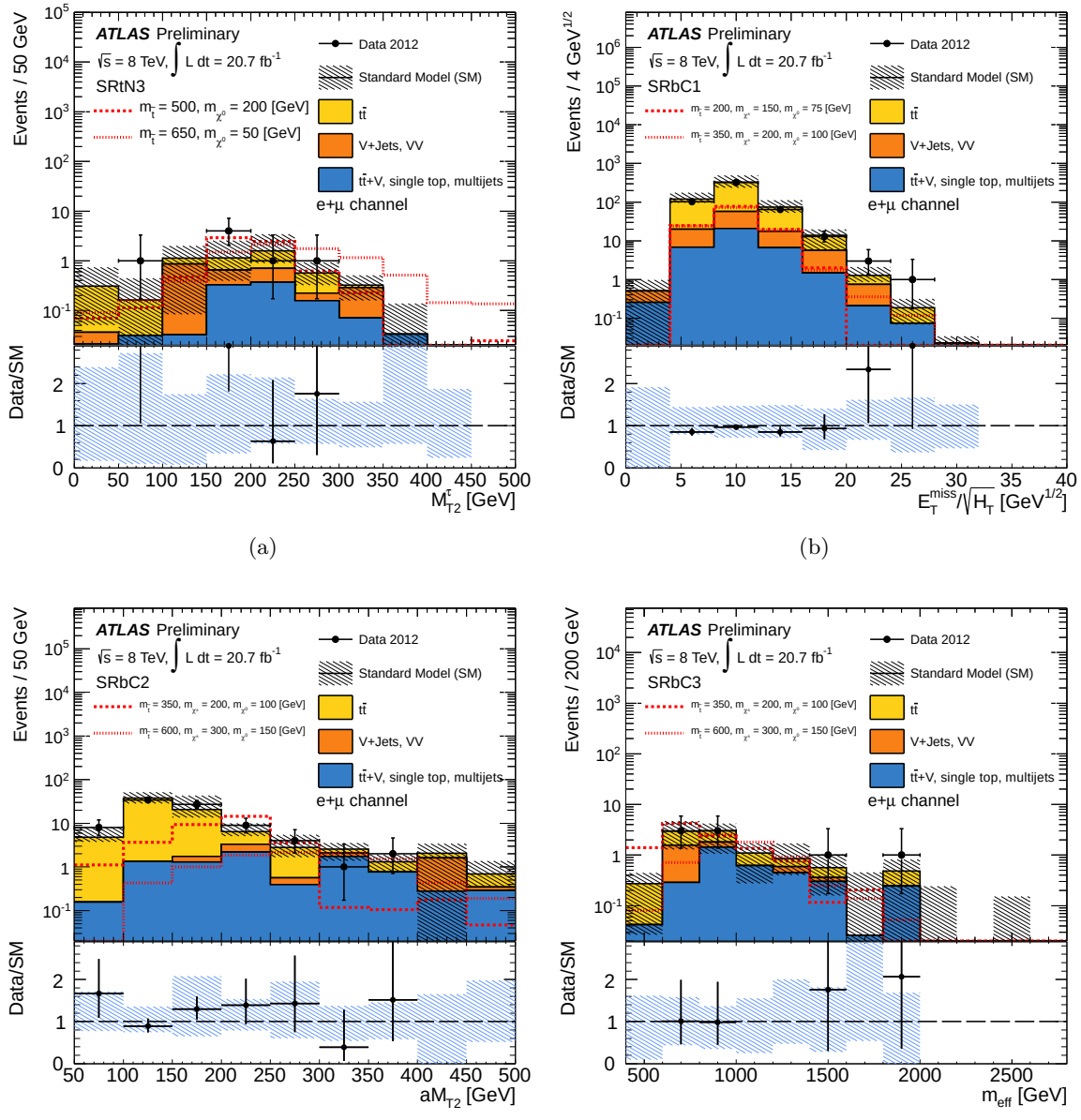

Figure 30: Characteristic E_t^{miss}- or M_T-distributions for the SR: SRtN3 (a), SRbC1 (b), SRbC2 (c) and SRbC3 (d)